EPJ Web of Conferences **44**, 03002 (2013)
DOI: 10.1051/epjconf/20134403002

Full potential calculations and atom in molecule analysis of the bonding properties of perovskites Borides XRh_3B (X=Dy, Ho, Er)

B. Lasri[1,2a], I. Merad Boudia[1], and T. Ouahrani[1,3]

[1] *Laboratoire de Physique Théorique, Université de Tlemcen B.P. 230, 13000 Tlemcen Algeria*
[2] *Université Dr Tahar Moulay de Saida, B.P. 138, Cité el Nasr, Saida (20000) Algeria.*
[3] *École Préparatoire en Sciences et Techniques, B.P. 230, 13000 Tlemcen Algeria*

Abstract. *ab initio* calculations were performed for the cubic perovskites Borides XRh_3B, (X=Dy, Ho, Er). In this work, we have used the augmented plane-wave plus local orbital method to compute the equilibrium structural parameters and electronic structure of densities of states, as well as for the first time, prediction of the thermo-elastic properties of these crystals are presented. The chemical bonding of these compounds has been investigated by using of topological analyses grounded in the theory of atoms in molecules (AIM). All of the electron density critical points in the unit cell were systematically calculated in order to calculate basins interaction of each atoms and give exact classification of the bonding character.

1 Introduction

Despite their name, rare earth elements are relatively plentiful in the Earth's crust, the proper quantification of dynamical, thermal, transition pressures and Clapeyron slopes... is critical for the interpretation of experimental data of these materials and for the construction of models of the Earth's interior [1, 2]. The modelling of materials from first-principles has taken a prominent role in the understanding of the interior of planets and in particular of the Earth, following the development of efficient *ab-initio* techniques with the increase in computer power.

Borides and carbides forming in the antiperovskite or perovskite structures as rare earth (R) rhodium borides RRh_3B_X [3] are technologically very important materials due to their high stability and hardness that make them very advantageous for applications in high temperature environment, cutting tools, superconductivity [4] and hard coatings. From their electronic structure the role of the $4f$ state in their chemical property can be important, as mentioned by Kojima *et al.* [5], the $4f$ states lie just above the Fermi level, there could be interesting changes in the properties under pressure. In such a case, leads to a change in a lattice parameter and in indirect way to the hardness of these crystals. Very recently, Djermouni *et al.* [6] have done a study on the magnetic stability of some carbides, they analyze their hybdridation of local magnetic moment and that according to the influence of the $4f$ state. Despite the published reports on this family compounds the investigation of $DyRh_3B$, $ErRh_3B$ and $HoRh_3B$ compounds is rarely invoked, apart the experimental measure from [7–9]. This

[a] e-mail: lasribo@yahoo.fr

implies the important role of theoretical analysis of fundamental features of electronic structure, electron density topology and bonding properties in these compounds under description, explanation and to some extent in prediction of thermal decomposition process pathway and its products.

A consistent, physically sound study of the chemical bonding in these compounds requires that extreme caution should be taken when using traditional orbital descriptions restated in the language of L/APW+lo. We have chosen, accordingly, the theory of atoms in molecules (AIM) of Bader [14] to overcome these difficulties and arbitrariness. It focuses on the electron density as the primary observable. This means that its conclusions are independent of the method chosen to obtain the density. It also allows us to directly calculate chemical bonding pictures coming from traditional wave function methods. On other hand, there is an additional point of interest, developments in the computation of first-principles phonon dispersion relations have led to an unprecedented accuracy in the prediction of thermodynamic properties within the harmonic approximation plus anharmonic corrections. For this propose we are aimed for the first time to investigate the thermal properties of the entitled compounds within the anharmonic Debey approximation as well as dynamical properties likes the equilibrium structures and the elastic constants.

The paper is organized as follows: we explain the computational method in Section 2. The results for the electronic structure dynamical and bonding properties are presented and discussed in Section 3. A brief conclusion is drawn in Section 4.

2 Theoretical method

To begin with the analysis of the electronic density and calculate the others dynamical properties, we need to know the equilibrium geometry of the compound.

To this end first principles calculations were carried by using of the new script RUNWIEN [10] interfaced to the WIEN2K package [11]. Atoms were represented by the hybrid full-potential (linear) augmented plane-wave plus local orbitals (L/APW+lo) method [12]. In this method wave functions, charge density, and potential are expanded in spherical harmonics within non-overlapping muffin-tin spheres, and plane waves are used in the remaining interstitial region of the unit cell. In the code, the core and valence states are treated differently. Core states are treated within a multi-configuration relativistic Dirac-Fock approach, while valence states are treated in a scalar relativistic approach. The exchange and correlation effects are treated by the Perdew-Burke-Ernzerhof generalized gradient approximation GGA [13].

3 Results and discussions

Great care has been taken to select the appropriate set of deformations involving changes in the cell lengths and angles to calculate the elastic properties of the studied compounds. This procedure implemented in RUNWIEN script, is based on performing a minimum number of finite Lagrangian deformations on the crystal unit cell. For cubic crystals, the mechanical stability requires the elastic constants satisfying the well-known Born stability criteria:

$$\begin{aligned} C_{11} &> |C_{12}| \\ C_{11} + 2 \times C_{12} &> 0 \\ C_{44} &> 0 \end{aligned} \tag{1}$$

From our calculated C_{ij} shown in Table 1, it is known that the perovskites $DyRh_3B$, $HoRh_3B$, and $ErRh_3B$ are mechanically stable. To the best of our knowledge, no experimental or theoretical data

Table 1. Equilibrium properties of calculated compounds: lattice constant, a; bulk modulus B; first derivative of the bulk modulus with respect to the pressure, B' and elastic constants C_{ij}(GPa). Our FPLAPW results using the PBE-GGA functional are compared to the experimental data.

	a (Å)	B (GPa)	B'	C_{11}	C_{12}	C_{44}
$DyRh_3B$	4.2089	173.6622	4.7643	283.185	104.809	38.731
	4.168					
	4.167					
$HoRh_3B$	4.2046	170.2477	4.9324	250.651	99.972	48.558
	4.151					
	4.160					
$ErRh_3B$	4.2026	174.3674	4.6777	260.589	127.687	53.381
	4.145					

for the elastic constants of these compounds are available. Therefore, we consider the present results as a prediction study.

A problem arises when single crystal samples cannot be obtained, for then it is not possible to measure the individual elastic constants C_{ij}. Instead, the isotropic bulk modulus B and shear modulus G are determined. These quantities cannot in general be calculated directly from the C_{ij}, but we can use our values to place bounds on the isotropic moduli. Reuss found lower bounds for all lattices, while Voigt discovered upper bounds [15]. For the specific case of cubic lattices, Hashin and Shtrikman [16] found stricter bounds. The isotropic bulk modulus for cubic system is given exactly by:

$$B_{V,R} = 1/3(C_{11} + 2C_{12}) \quad (2)$$

$$G_V = 1/5(C_{11} - C_{12} + 3C_{44}) \quad (3)$$

$$G_R = [5C_{44}(C_{11} - C_{12})]/[4C_{44} + 3(C_{11} - C_{12})] \quad (4)$$

The shear modulus G is given by

$$G = (G_V + G_R)/2 \quad (5)$$

Which are frequently measured for polycrystalline materials when investigating their hardness, the Young's modulus E and the Poisson's ratio σ:

$$E = 9BG/(3B + G) \quad (6)$$

$$\sigma = (3B - E)/6B \quad (7)$$

The value of the Poisson ratio for covalent materials is small ($\sigma \approx 0.1$), whereas for ionic materials a typical value of σ is 0.25 [17]. In our case the value of σ vary from 0.351 ($DyRh_3B$), 0.329 ($HoRh_3B$), to 0.348 ($ErRh_3B$), i.e. according to this index, a higher ionic contribution in intra-atomic bonding for these compounds should be assumed. However, this tool still does not give good results in all cases, for instance in our previous work [26], this index has been predicted that our compounds have strong ionic behaviour, but after its more reliable analysis by means of the QTAIM theory, we have found that the character must place our crystals rather on the covalent to ionic edge, closer to the covalent than to the ionic corner. Our results reveal that the three studied compounds have Young modulus for Dy, Ho and Er crystals, equal to 54.49, 57.94 and 58.27 (GPa) respectively, it means that the rigidity rises with the increase of the atomic number.

The investigation of the Debye temperature is usually calculated from micro-hardness [18], melting point [19] and also using elastic constants [20] or simply with empirical relations between Θ_D and the plasmon energy [22]. In this work, we have used the quasi-harmonic Debye approximation

Table 2. Selection of thermal properties at 300 K: thermal expansion coefficient (α, 10^{-5} K^{-1}); vibrational contribution to the volume and pressure constant heat capacities (C_v and C_p in J/mol K); isothermal and adiabatic bulk moduli (B and B_S, in GPa); Debye temperature (Θ_D, K); and Grüneisen parameter (γ).

Crystal	α	C_v	C_p	B	B_S	Θ_D	γ
$DyRh_3B$	4.82	118.66	123.47	151.45	157.58	300.98	2.801
$HoRh_3B$	4.44	119.87	152.87	113.47	125.01	268.41	5.570
$ErRh_3B$	4.67	118.57	123.11	152.88	158.73	303.25	2.730

[23]. This latter is well detailed in much work [24], so we will just have to give the most important properties at ambient temperature. A set of properties that are specially related to the volume and dependent to Debye temperature Θ, as the heat capacities, thermal expansion coefficient, isothermal and adiabatic bulk moduli, Grüneisen parameter and obviously the Debye temperature. all these quantities are gathered in Table 2.

3.1 Density of states and population analysis

In this part, the electronic structure and population analysis features are discussed. When we observe carefully the topology of curves and especially related to the f states, the magnetic character seems clear, however, after analysis we made sure that they are ferromagnetic and not anti-ferromagnetic materials, after reversing of the spin the shape of the densities remain the same. However, this work does not address the magnetic properties, so we pay more attention to the electronic structure. In order to have more understanding and give weight interpretation of this structure, we start by analysing the Mulliken charge population, this procedure is very simple as it is implemented in the CASTEP code, it has not the same reliability as the sophisticated method proposed by Bader, however, we can see through the Table 3: the vast majority of the electrons comes from the character d states of rhodium atom and from the f states of rare earth elements. We have analyzed the contribution of the anion and cation's states to each set of bands by decomposing the total density of states (Total Dos) (see Fig. 1a) into s-, p-, d-, and f-orbital contributions. The result is the site-projected partial density of states shown in Figure 1b,c,d. As a consequence of similarity between the calculated spectrum of the three compounds, we show only the plot of the spin-polarized electronic structures of the $DyRh_3B$ crystal, it will be done as a demonstrator.

We may see that there is a number set of pronounced peak formed essentially between -10 and 10 eV. The bands originate predominantly from the B and Rh of s, p or d states, are similar in the two state of the spin. Nevertheless, a sharp peak originated from the Dy-f state are located at -4 eV in the spin up order and centred at the energy Fermi in the spin down order. Dy-p character are shifted in the different order of the spin by about 1.5 eV. As conclusion the electronic structure is found to be metallic with the near-Fermi-level DOS determined by the Dy 4f, Rh 4d, and B 2p states.

3.2 Electronic density topology

The definition of a crystalline electro-negativity is intimately bounded to the possibility of splitting the crystal properties into atomic contributions. One opportunity to resolve this problem is the calculated electron density (ρ) of the system. Because of the steep behaviour of ρ we have redone the calculation under some more strict conditions: namely, the FP-LAPW parameters $R_{mt}K_{max} = 9.0$, in the same time we have takes care our analysis by considering density grid with a dense mesh to avoid problems with critical points localization. The electron densities calculated from the RUNWIEN calculations have been taken as input to the CRITIC program [25], a code that searches for all the independent critical points

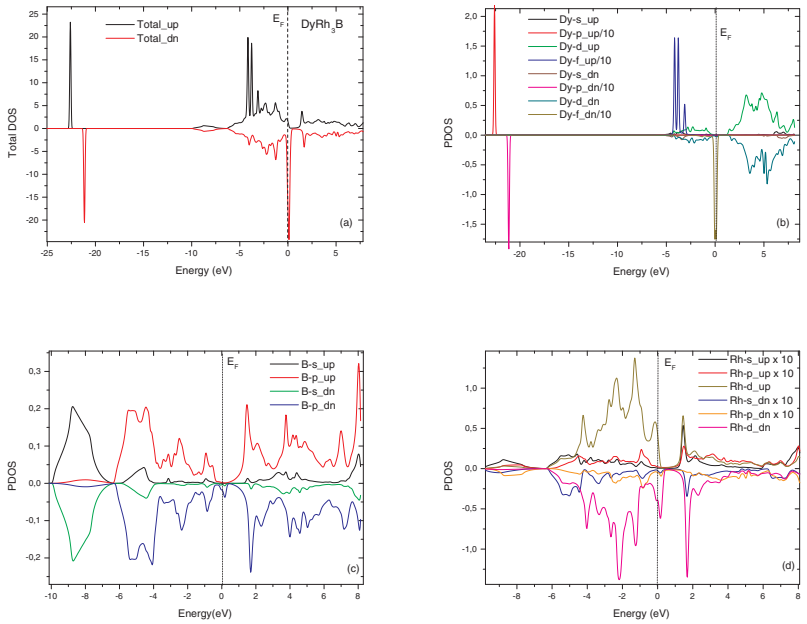

Figure 1. Spin polarized calculation of the total and partial densities of states of the $DyRh_3B$ crystal

Table 3. Atomic Populations (Mulliken)

Species	Ion	*s*	*p*	*d*	*f*	Total	Charge (e)
$DyRh_3B$							
B	1	1.76	1.45	0.00	0.00	3.20	-0.20
Rh	1	0.80	0.24	8.40	0.00	9.44	-0.44
Rh	2	0.80	0.24	8.40	0.00	9.44	-0.44
Rh	3	0.80	0.24	8.40	0.00	9.44	-0.44
Dy	1	2.58	4.01	2.10	9.77	18.47	1.53
$HoRh_3B$							
B	1	1.31	2.25	0.00	0.00	3.57	-0.57
Rh	1	0.94	0.26	8.25	0.00	9.45	-0.45
Rh	2	0.94	0.26	8.25	0.00	9.45	-0.45
Rh	3	0.94	0.26	8.25	0.00	9.45	-0.45
Ho	1	2.81	4.19	1.49	10.59	19.07	1.93
$ErRh_3B$							
B	1	1.32	2.26	0.00	0.00	3.57	-0.57
Rh	1	0.94	0.23	8.25	0.00	9.42	-0.42
Rh	2	0.94	0.23	8.25	0.00	9.42	-0.42
Rh	3	0.94	0.23	8.25	0.00	9.42	-0.42
Er	1	2.82	4.31	1.45	11.60	20.18	1.82

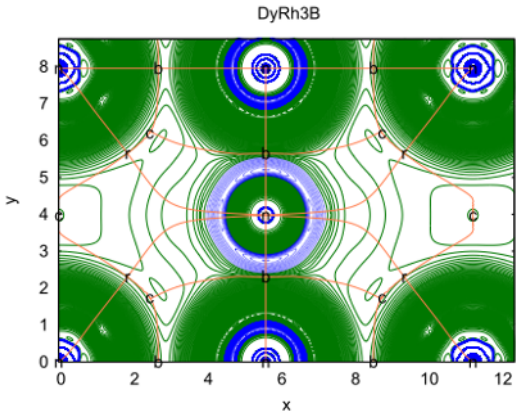

Figure 2. Electron density of $DyRh_3B$ in the [111] plane. This plane contains all the CPs of the structure: the three nuclei, the B–Rh and Dy–Rh bond Cp's, a single ring Cp's, and two different cage Cp's.

(see Figure 2). This task, computationally cheap, corresponds to the determination of the primary bundles or the atomic basins and the integration of quantum mechanical properties within them. That means to find a solutions to the equation $\vec{\nabla}\rho \cdot \vec{n} = 0$. This method, previously described in ref [26, 27], is based on the recursive division of the irreducible wedge of the Wigner-Seitz polyhedron of the Bravais lattice and the minimization of $|\vec{\nabla}\rho|$ within the edges, surfaces, and interiors of the resulting tetrahedra. Using the critical points distribution shown in the plot of the $\{111\}$ plane of the charge density in figure 2, and according to the structure satisfying Euler's relationship (faces − edges + vertices=2), we can construct in this manner a polyhedra which contains all atomic attraction basins (see Figure 3). From these quantities and using the relation given the ionicity index defined as an average for all the basins of the ratio between the local topological charge and the nominal oxidation state, $c = \frac{1}{N}\sum_{\Omega=1}^{N} \frac{Q(\Omega)}{OS(\Omega)}$, and the flatness topological indices $fa = \rho_c^{min}/\rho_b^{max}$ given the percentage of the metallic character, all these index are gathered in Table 4.

On 120 halide perovskites, Luaña *et al.* [28] have found that the electronic density can be classified into one of seven different topological schemes (i.e. seven different arrangements of critical points). Our investigated compounds according to figure 3 correspond to the dominant $\mathcal{R}9$ family [28]. where the Boride basin is topologically equivalent to a cube. The result from calculating the two indices of the metallic behaviour fa and $1 - c$ giving the degree of covalency predicted that our materials are dominated by nearby 65 % by covalent character with a mixture of 17 % of metallic one.

Visualizing the arrangements of critical points and the connections between them is not an easy task given the huge number of points that lie within the unit cell. The most significant and comprehensive form that we have found is by depicting the attraction basins for each nuclei displayed in Figure 3 and 2. It can be easily shown that site symmetry determines that some special positions of the cell must be CP's of the electron density. This is the case for the Wyckoff's 1a, 1b and 3c positions in the Pm3m space group of the perovskites. From another point of view, note that in such crystals, for the case of XRh_3B compounds, the B anion alloying generally creates strain in the lattice and displaces the nearest Rh ions leading to an increase in lattice parameter. The analysis of charge population has given the values of -2.20, -1.54 and -1.35 for the bonds Dy–Rh, Ho–Rh and Er–Rh respectively, resulting on direct covalent interaction between them.

Table 4. Atomic properties of XRh_3B (X=Dy, Ho, Er) In column order, it shows the multiplicity in the conventional unit cell, the integrated charge Q, the degree of ionicity c and the flatness topological indices fa.

Atom	Wyck.	Q	c	fa
$DyRh_3B$			33.85%	17.46%
Dy	1a	+1.3676		
B	1b	−0.1309		
Rh	3c	−1.2367		
$HoRh_3B$			34.19%	17.25%
Ho	1a	+1.3809		
B	1b	−0.1316		
Rh	3c	−1.2492		
$ErRh_3B$			34.41%	17.23%
Er	1a	+1.3879		
B	1b	−0.1299		
Rh	3c	−1.2579		

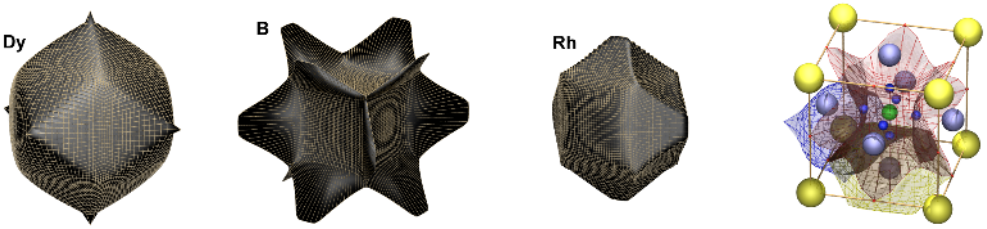

Figure 3. Top: atomic basins for Dy , Rh and B in the $DyRh_3B$ Perovskite, Bottom: Crystallographic (balls and sticks) of $DyRh_3B$ crystals. Yellow balls represents the dysprosium ions, Light blue balls rhodium ions and green balls Bore ions. Small red balls are placed at the Wycko's 3c are the (3,-1) bond Cp's and (3,3) cage Cp's are represented by the small blue balls

4 Conclusion

In summary, our *ab initio* simulation provides valuables information regarding dynamical, electronic and bonding properties of the borides rare earth perovskites with formula XRh_3B, where X= Dy, Ho as well as Er.

In the same time evaluation for the first time of elastic and thermal quantities have been provided. The stability of these compounds are found from this dynamical properties. We have presented also an analysis of the most common behaviour of the electronic structure of the densities of states, as a consequence of the behaviour discussed above, the f state is located very close to the Fermi level, this makes our ferromagnetic materials very matchmaker for an application in the field of superconductivity.

Additionally, by means of AIM theory we have provided partition of atomic charge densities. The atomic basins of our crystals contain a substantial net charge, the analysis of the electron density has enabled a thorough characterization of electron pairing in ionic bonds. We have further exploited this information to predict exact classification of the character bonding. Our components are rather covalent than ionic with a mixture of metallic character.

References

[1] Wentzcovitch, R. M., Wu, Z. and Carrier, P. (2010), vol. 71 of Reviews in Mineralogy & Geochemistry, pp. 99–128, Mineralogical Soc. Amer., Chantilly, VA, USA.

[2] Wentzcovitch, R. M., Yu, Y. G. and Wu, Z. (2010), vol. 71 of Reviews in Mineralogy & Geochemistry, pp. 59-98, Mineralogical Soc. Amer., Chantilly, VA, USA.

[3] H. Holleck, J. Less-Common Met. **52**, 167 (1977)

[4] M. Oku, T. Shishido, T. Shinohara, T. Fukuda, Q. Sun, Y. Kawazoe, K. Wagatsuma Journal of Alloys and Compounds **339**, 317–326 (2002)

[5] H. Kojima, R. Sahara, T. Shishido, A. Nomura K. Kudou, S. Okada, V. Kumar, K. Nakajima and Y. Kawazoe Appl. Phys. Lett. **91**, 081901 (2007)

[6] M. Djermouni, S. Kacimi, and A. Zaoui, Phys. Status Solidi b, **248** 8 (2011)

[7] M. Takeda, J. Wang, M. Takahashi, T. Shishido, A. Yoshikawa , A. Nakamura Journal of Alloys and Compounds **408–412**, 371-374 (2006)

[8] H. Takei, T.Shishido, Journal of the Less-Common Metals **97**, 223-229 (1984)

[9] R. Vijayaraghavan, Journal of Magnetism and Magnetic Materials **47**, 561-566 (1985)

[10] A. Otero-de-la Roza, V. Luaña, Comput. Phys. Commun. **108**, 800-812 (2009).

[11] Blaha P, Schwarz K, Madsen G K H, Kvasnicka D and Luitz J 2001 WIEN2K, An Augmented Plane Wave +Local Orbitals Program for Calculating Crystal Properties, Karlheinz Schwarz, Techn. Universitat, Wien, Austria (ISBN 3-9501031-1-2)

[12] E. Sjöstedt, L. Nordstrom, and D. J. Singh, Solid State Commun. **114**, 15 (2000).

[13] J. P. Perdew, K. Burke, M. Ernzerhof, Phys. Rev. Lett. **77**, 3865-3868 (1996)

[14] Bader, R. F. W. Atoms in Moleculess, A Quantum Theory, Oxford University Press: Oxford, (1990).

[15] M.J. Mehl, B.M. Barry, D.A. Papaconstantopoulos, in: J.H. Westbrook, R.L. Fleischeir (Eds.), Intermetallic Compounds: Principle and Practice, Volume I: PrinciplesWiley, London, pp. 195-210 (Chapter 9) (1995).

[16] Z. Hashin, S. Shtrikman, J. Mech. Phys. Solids **10**, 335 (1962).

[17] J. Haines, J. M. Leger ,G. Bocquillon, Annu. Rev. Mater. Res. **31**. 1 (2001)

[18] S. C. Abrahams, F. S. L. Hsu, J. Chem. Phys. **63**, 1162 (1975).

[19] B. N. Oshcherin, Phys. Stat. Solidi (a) **35**, K35 (1976).

[20] H. Siethoff, K. Ahlborn, J. Appl. Phys. **79**, 2968 (1996).

[21] C. Rincon, Phys. Stat. Solidi (a) **134**, 383 (1992).

[22] V. Kumar, A.K. Shrivastava, Rajib Banerji, D. Dhirhe, Solid State Communications **149**,1008–1011 (2009).

[23] M. A. Blanco, E. Francisco, V. Luaña, Comput. Phys. Commun. **158**, 57 (2004).

[24] T. Ouahrani, A. Otero-de-la-Roza, R. Khenata, Luaña, B. Amrani, Computational Materials Science **47**, 655-659 (2010)

[25] A. Otero-de-la-Roza, M. A. Blanco, A. Martín Pendás and V. Luaña, Comput. Phys. Commun. **180**, 157 (2009).

[26] T. Ouahrani, A. Otero-de-la-Roza, A.H. Reshak, R. Khenata, H.I. Faraoun, B. Amrani, M. Mebrouki and V. Luaña, Physica B **405**, 3658–3664 (2010)

[27] A. Otero-de-la-Roza and V. Luaña, J. Chem. Theory Comput. **6**, 3761–3779 (2010).

[28] V. Luaña, A. Costales, and A. Martín Pendás, Phys. Rev. B **55**, 4285 (1997).